

Compliant Terrain Legged Locomotion Using a Viscoplastic Approach

Vasileios Vasilopoulos, *Student Member, IEEE*, Iosif S. Paraskevas,* *Student Member, IEEE* and Evangelos G. Papadopoulos,** *Senior Member, IEEE*

Abstract— Legged locomotion is a rapidly advancing area in robotics, yet still a large number of open questions exist. This work focuses on the foot-terrain interaction and its effect on the motion of a one-legged system. This interaction is usually tackled by disregarding some of the effects of ground deformation like permanent deformation and compaction. Inspired by other areas of engineering, an impact dynamics model is developed, allowing a more thorough study of the behavior during fast dynamic walking. This approach can be regarded as a viscoplastic one. The monopod controller presented in previous work is extended to cope with deformable terrains, based on energy dissipation considerations, without requiring the knowledge of the ground parameters. Simulation results prove the validity of the theory presented.

I. INTRODUCTION

A central goal in the field of legged robotics is the development of machines able to traverse rough terrain, which wheeled vehicles cannot access. However, such machines are subject to more complex control requirements. The problem is exacerbated when running on terrain with unknown properties. Earlier approaches required a known type of terrain, to be traversed with a statically stable gait, hence simplifying control and stability issues [1]. Other works focused on bipeds running over stair-like terrain, e.g. [2]. Recent developments towards the running on unknown terrains like the RHex and BigDog robots, have been demonstrated [3] and [4]. However, the RHex uses open-loop control, thus forward speed is not controlled tightly.

Despite progress made in dynamic models and control methods for legged robots, many notable studies disregard the importance of foot-terrain interaction. For example, for the two-link monopod the contact point between the foot and the ground was modeled as a completely stiff revolute joint [5]. A similar approach for the dynamic representation of a monopod hopping robot was proposed in [6], where a control method that can render the robot able to traverse rough terrain using a single actuator was presented. In fact most efforts in the literature consider the terrain as nondeformable.

To cope with the foot-terrain interaction, a reliable representation of the ground is needed as the terrain deformation affects leg motion, while energy is dissipated. Usually a simplified ground model is chosen, and controllers cope with any deviations considering them as disturbances. However this does not ensure success in highly deformable environments. Some works account for a foot-ground interaction employing terramechanics, e.g. [7], making use of Bekker or similar models [8]. Yet, this approach does not always result in an accurate representation of foot-terrain dynamic interaction, for which the term “*terradynamics*” is coined [9]. The approach in [9] is interesting for the locomotion of the robots examined but does not include the impact characteristics, prominent in fast dynamic walking.

In principle, impacts can be modelled via three methods [10]. The *stereomechanical theory* is not very accurate, while *FEM methods* are computationally demanding and difficult to use in online algorithms. The use of *compliant (viscoelastic) models* is the most appropriate, as different soils can be simulated by lumped parameters with suitable characteristics. More details can be found in the literature, e.g. [11]. In other engineering areas viscoplastic extensions of these models are proposed, e.g. [12]. In our work, the viscoelastic impact models are modified appropriately for use in robotics, in this case in simulating the terrain behavior, e.g. as shown in [8], therefore a viscoplastic approach is employed. An earlier work on this showed its potentials [13].

This work studies the effects of foot-terrain interactions in legged robots and methods to cancel them out. The adverse effects of terrain deformation during motion are illustrated. A new model for impact dynamics is developed, allowing the study of the behavior of fast dynamic walking for a monopod robot. Using response feedback, a new controller is developed by modifying a controller from our previous work, able to maintain desired apex height and speed with a single actuator and in the presence of unknown dissipative terrains. Simulation results show that the developed controller overcomes terrain variations, and achieve gait objectives.

II. BACKGROUND ON MONOPOD CONTROL

Fig. 1a shows a single-actuator hopping monopod robot.

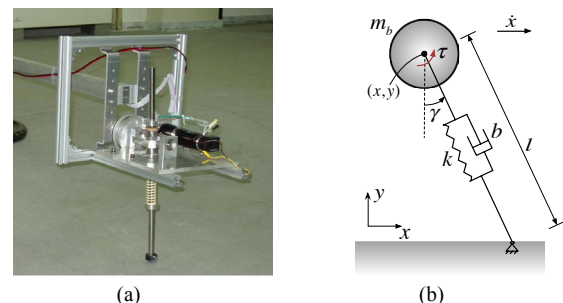


Figure 1. (a) Experimental setup of monopod and (b) monopod's 2D model.

*Mr. Paraskevas has been co-financed by the European Union (European Social Fund – ESF) and Greek national funds through the Operational Program “Education and Lifelong Learning” of the National Strategic Reference Framework (NSRF) - Research Funding Program: Heracleitus II. Investing in knowledge society through the European Social Fund.

**Prof. Papadopoulos has been co-financed by the European Union (European Social Fund-ESF) and Greek national funds through the Operational Program “Education and Lifelong Learning” of the National Strategic Reference Framework Research Funding Program: THALES: Reinforcement of the interdisciplinary and/or interinstitutional research & innovation.

The authors are with the Department of Mechanical Engineering, National Technical University of Athens, 9 Heroon Polytechneiou Str., 15780 Athens, Greece. (e-mails: vasilis.vasilop@gmail.com; isparas@mail.ntua.gr; egpapado@central.ntua.gr; ph.: +30-210-772-1440).

This robot is used in our laboratory as a leg testbed for multi-legged robots. A novel MultiPart controller (MP) for this robot that can control both the apex height and the forward velocity with a single actuator at the hip was proposed in [6] and [14]. The behavior of the robot was tested and validated using an experimental setup, which consists of a central pivot, and an arm that allows the robot to perform a circular motion, with constraints on pitching.

The robot is modeled as a body of mass m_b , which includes the main body mass and partly the supporting arm mass, with a springy leg, as shown in Fig. 1b. The free length of the leg is L , the stiffness of the linear spring is k , and the torque applied by the single actuator is τ . The angle of the leg with respect to the vertical is γ and its instant length at any time is l . The energy losses due to viscous friction in the leg prismatic degree of freedom (dof) are modeled by a damping coefficient b , while the leg mass is considered negligible. During stance and assuming a stiff ground with appropriate friction, the ground interaction is modeled using a revolute joint. The equations of motion during the stance and flight phases can be found in [6] and [14]. During flight, the system is assumed to perform a ballistic trajectory.

Controlling the apex height is important when running on unknown terrain, allowing the foot to maintain a specific clearance from the ground, thus avoiding sudden discontinuities (e.g. rocks). The controller determines a touchdown angle to achieve the desired apex height, and applies a constant torque during stance to achieve the desired forward speed. Thus, the MP tries to maintain a passive gait with desired characteristics by applying proper actuation to compensate for energy losses. This approach results in minimum energy consumption, but requires an estimate of the leg compliance and system losses.

During the flight phase (f), the desired touchdown angle γ_{td} to achieve a specified apex height is calculated as

$$\gamma_{td} = f(\text{state at liftoff}, \dot{x}_{des}, h_{des}) \quad (1)$$

where \dot{x}_{des} and h_{des} are the desired forward speed and apex height respectively. The robot leg is servoed to the desired angle using a simple proportional derivative (PD) controller. The control torque applied by the actuator is then,

$$\tau_f = k_p \cdot (\gamma_{td} - \gamma) + k_d \cdot (-\dot{\gamma}) \quad (2)$$

where k_p and k_d are controller gains. The values of $k_p = 150$ and $k_d = 2.4$ have been selected and used in both simulations and experiments, in order for the controller to be both fast enough to change the leg angle before the next touchdown, while avoiding overshooting and unwanted oscillations. The necessary control torque that must be applied during the stance (s) phase, is

$$\tau_s = g(\text{state at liftoff}, \dot{x}_{des}, h_{des}, \gamma_{td}) \quad (3)$$

At the end of the flight, the next stance begins, the constant torque τ_s is applied, and the cycle repeats itself. In Fig. 2 the motion of the monopod using the MP on a nondeformable ground is presented. Although the response of the MP controller satisfies the desired gait targets, it relies on the assumptions of an ideal massless foot and of an interaction with a stiff ground that can be modeled by a revolute joint. This is common for most legged robot controllers. In the next sections, the assumptions of a stiff ground and massless foot are dropped, and the effects on the controller performance and gait characteristics are studied.

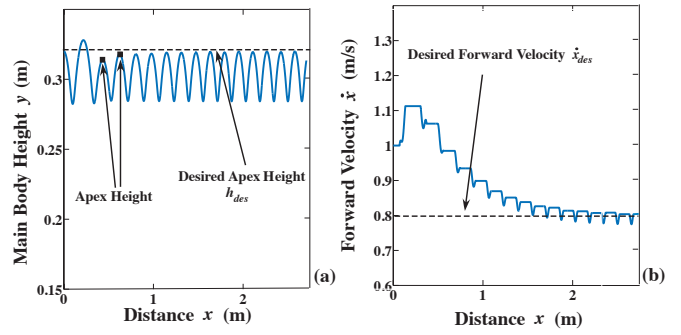


Figure 2. Use of MP on a nondeformable ground: (a) Apex height and (b) Forward velocity.

III. IMPACT MODEL FOR A DEFORMABLE TERRAIN

The model of the foot-terrain interaction must represent realistically the motion behavior while running on deformable terrains. The main parameters that affect the motion are the compliance of the ground (e.g. running on cement versus running on sand), the depth of the permanent deformation that may occur (e.g. running on clay versus running on sand) and the change of characteristics due to repetitive loading on a particular point (i.e. compaction or similar phenomena). In a standard terramechanics approach, it is assumed that a wheel or a foot are in touch with the ground for considerable time, or permanently. This approach cannot be applied to the case of fast dynamic walking. A way to incorporate the elastoplastic behavior of the ground is by using an extension of non-linear viscoelastic models, called *viscoplastic*. In this work, viscoplasticity is used to examine the dynamic interaction between the foot and the ground, a method which is an alternative to the *terramechanics* and the *terradynamics* approaches. However it must be noted that in granular media, where impact forces are of hydrodynamic nature, the proposed model may be inappropriate.

In viscoelastic theory, a compliant surface can be modeled by a combination of lumped parameter elements (springs and dampers). Some common impact models include the Kelvin-Voigt (KV) and the Hunt-Crossley (HC) [11]. The latter model shall be used as a reference as it provides a good initial description of the interaction. According to the HC model, the interaction force F_g is

$$F_g(y_g, \dot{y}_g) = k_g \cdot y_g^n + b_g \cdot \dot{y}_g \cdot y_g^n \quad (4)$$

where k_g and b_g are the stiffness and damping coefficients respectively, n in the case of Hertzian non-adhesive contact is equal to 1.5, and y_g is the depth of penetration (positive towards the ground). The parameter k_g represents the equivalent stiffness between the materials that come into contact (i.e. foot and terrain) [15]. Damping is considered as a parameter affected by the stiffness [16], and is given by

$$b_g = 1.5 \cdot c_a \cdot k_g \quad (5)$$

where c_a is usually between 0.01-0.5 depending on the materials and impact velocity. Throughout this work we use $c_a = 0.2$ without affecting the generality of the conclusions.

Existing viscoelastic models implicitly assume that the impact starts and ends at $y_g = 0$, i.e. that no permanent deformation applies. However, this is not true in general. Also according to viscoelastic models, the terrain behavior under repetitive loading or compaction is not modelled. Examining closely the ideal case (id), in which the impact

(stance in this case) starts and ends at $y_g = 0$, one assumes that the robot clears the ground at the end with some spring elongation $l_{id,e}$ (i.e. equal to the momentary length of the leg). On a nonideal (nid) deformable ground however, the robot shall clear the ground at $y_g > 0$ due to terrain permanent deformation; the final elongation $l_{nid,e}$ will be in general $l_{nid,e} \neq l_{id,e}$. Thus a different approach is required.

Assuming a *viscoelastic* model, such as the HC, suppose that a body impacts the ground, Fig. 3a. During compression, both the interaction force and depth increase, and the relative velocity decreases. When the foot velocity is zeroed, i.e. $\dot{y}_g = 0$, the maximum compression $y_{c,max}$ has been reached. During the restitution phase, the foot velocity increases but in the opposite direction and the depth and the interaction force decrease. The restitution ends when both the depth and the interaction force are zeroed, but in fact this is due to the closed form of the impact models. The key event is that the interaction force is zeroed, i.e. there is no more contact between the impacting body (impactor) and the terrain.

Studying the behavior of terrains using experimental data, as for example in [8], it is obvious that the deformable nature of the terrain is not described accurately with such a model. Yet the strict viscoelastic description of the process can be extended in the case of plastic deformation via appropriate lumped elements (viscoplastic description). This work proposes a model that treats the impact piecewise, Fig. 3b.

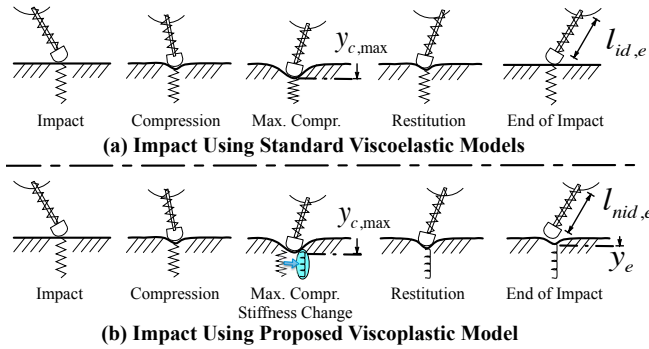


Figure 3. Impact models (a) Standard viscoelastic and (b) Proposed viscoplastic.

According to the proposed model, the compression phase is the same to that in the viscoelastic case. During this phase, part of the energy is stored in the (fictitious) spring, which represents the interaction stiffness, another part is dissipated through material internal losses (represented by damping b_g) and a last part is dissipated during terrain shape deformation (e.g. due to cratering around the impact point or compaction). As restitution is reached, material in the direction of motion has been displaced due to the deformation and/or the terrain becomes stiffer because of compaction. Then the spring, which represents the interaction stiffness, cannot be extended to its initial height (i.e. $y_g = 0$). The restitution phase will be shorter and the spring stiffer. Thus there is strong non-linearity between compression and restitution, which takes the form of a piecewise equation.

The interaction force F_g at instance i is modeled as,

$$F_g^i(y_g, \dot{y}_g) = \begin{cases} F_c^i = (\lambda_c^i \cdot k_g + b_g \cdot \dot{y}_g)(y_g - y_e^{i-1})^n, & \dot{y}_g \geq 0 \\ F_r^i = (\lambda_r^i \cdot k_g + b_g \cdot \dot{y}_g)(y_g - y_e^i)^n, & \dot{y}_g < 0 \end{cases} \quad (6)$$

where the subscript c stands for compression and r for restitution, and y_e is the depth at the end of impact (see Fig. 3b). To account for successive impacts on the same horizontal point, the index i is used to identify an impact instance, as the terrain inherits the characteristics from the previous instant due to permanent deformations. The latter are expressed with the *Coefficient of Permanent Terrain Deformation* λ , which has a recursive form

$$\lambda_c^i = \begin{cases} 1, & i=1 \\ \lambda_r^{i-1}, & i>1, i \in \mathbb{N} \end{cases} \quad (7)$$

$$\lambda_r^i = \lambda_r^i(\text{materials, velocity, } i), \quad i \in \mathbb{N}$$

Since the ground spring is stiffer during restitution than in compression, $\lambda_r^i \geq \lambda_c^i \geq 1$. Typically, as the same horizontal position (contact point) is compressed, it becomes stiffer, therefore in this work the following model is proposed,

$$\lambda_r^i = 1 + a(i) \cdot (1 - e^{-i\beta(i)}), \quad i \in \mathbb{N} \quad (8)$$

where $a(i)$, $\beta(i)$ are functions which also depend on materials and velocity. This exponential function gives larger permanent deformations during the first impacts. Note that if $a(i)=0$ or $\beta(i)=0$, (6) reduces to the HC model. Parameter a sets the maximum value of λ_r^i , whereas an increase in β increases the speed of reaching this value. Fig. 4 illustrates (6), i.e. the impact force as a function of penetration depth for various λ , in the case of a 1kg ball falling with zero velocity from 0.5m height to a surface with $k_g = 8 \cdot 10^4$ N/m.

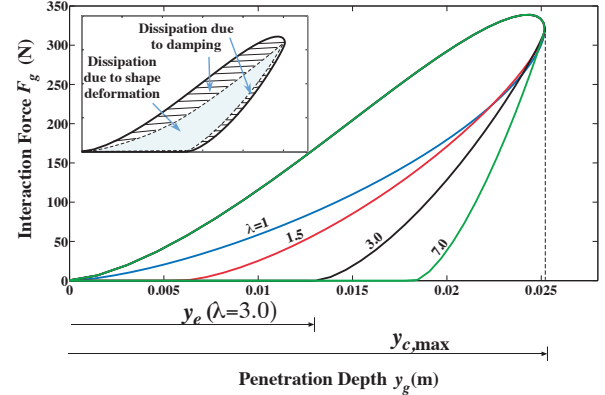


Figure 4. Impact curves for the proposed impact model (6) for various λ . The inset shows the corresponding distribution of the dissipated energy.

In the inset of Fig. 4 the distribution of the energy dissipation is presented. Note that for clarity fixed values of λ were used in Fig. 4 (i.e. (8) was not used).

The final depth y_e^i can be calculated by observing that at the maximum compression $y_{c,max}^i$ the following applies

$$y_{c,max}^i \Leftrightarrow F_c^i = F_r^i \quad \text{and} \quad \dot{y}_g = 0 \quad (9)$$

and using (6) one can deduce

$$y_e^i = y_{c,max}^i \cdot \left(1 - \sqrt{\lambda_c^i / \lambda_r^i}\right) + y_e^{i-1} \cdot \left(\sqrt{\lambda_c^i / \lambda_r^i}\right) \quad (10)$$

where $y_e^0 = 0$ for consistency.

It is very interesting to study the impact behavior of a more complex system of bodies like the robot on Fig. 6, while it falls vertically. As the foot mass comes into contact

with the ground, the phases of compression and restitution occur. However the upper mass due to its larger inertia and leg compliance, continues its downward motion and thus the forces which act on the lower mass by the spring (and damper) and the ground interaction can be equal before the system clears the ground, therefore a “recompression” phase starts (impact instance $i+1$). This can be repeated many times until the system as a whole clears the terrain, and the stance (i.e. the impact) is considered over. In Fig. 5 the interaction force versus the penetration depth is presented for such a case on a very stiff ground ($k_g = 10^6$ N/m), where the upper and lower masses are 4kg and 0.1kg respectively, length of the leg $L=0.30$ m and spring and damper parameters $k=12,000$ N/m and $b=0$ Ns/m. Equation (8) is used with $a=0.5$ and $\beta=1$. The system falls from 1cm height with no initial velocity.

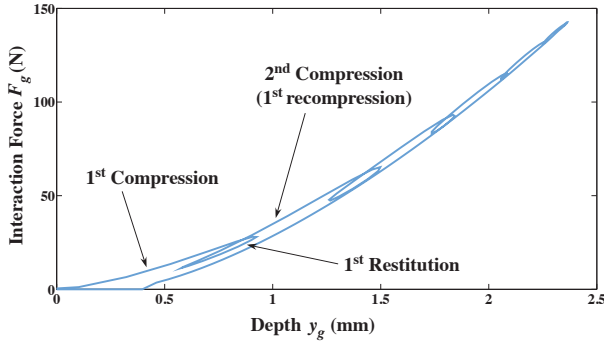


Figure 5. Impact curve for a case with many recompressions.

Discussion. (a) An advantage of the developed model is that it can be used for repetitive loading by increasing the impact instance index i for a particular contact point. A special case of repetitive loading is when the impactor is a multibody system, such as a legged robot. (b) This model is arithmetically stiff. Depending on the complexity of the problem to solve, high accuracy in Matlab may be required, (c) The use of the HC model as a basis in (6) is purely a matter of choice; the core ideas of the developed model are also applicable to other viscoelastic models, (d) proper selection of λ can describe complex phenomena, and (e) due to the previous reasons, this is a very general impact model.

IV. EXTENDED SYSTEM MODEL AND CONTROL

The foot is no longer considered massless during the stance or flight phase and a more detailed model is developed. The goal is to make the controller cope with terrain compliance and deformation. It is assumed that: (i) the foot is a point mass, i.e. a point contact occurs each time the foot impacts the ground, (ii) during stance, the foot motion is constrained in the horizontal direction, i.e. static friction is able to prevent the foot from slipping. To ensure this, a restriction of ± 15 deg on the angle range is implemented, (iii) bulldozing can be neglected, and (iv) the actuator is torque limited.

Model Development. The model shown in Fig. 6, consists of a mass M describing an effective mass due to the robot body and to part of the experimental setup, and a mass m describing the effective mass of the robot leg and foot. The rest of the symbols are the same to those in Section II. The force from the ground (F_g) is calculated using (6). During

the flight phase $F_g = 0$; a controller is used to position the leg at the desired touchdown angle given by (1).

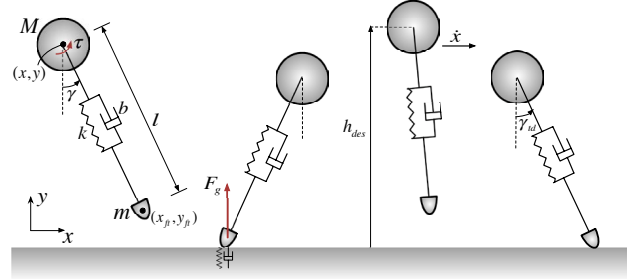


Figure 6. Model of one-legged robot under examination.

The system variables for the *flight phase* are the coordinates of the main body x, y and the coordinates of the foot x_{ft}, y_{ft} . The equations of motion become (with $s\gamma = \sin\gamma$ and $c\gamma = \cos\gamma$)

$$M \cdot \ddot{x} + k \cdot (L-l) \cdot s\gamma - b \cdot \dot{l} \cdot s\gamma = -\tau_f \cdot l^{-1} \cdot c\gamma \quad (11)$$

$$M \cdot \ddot{y} + M \cdot g - k \cdot (L-l) \cdot c\gamma + b \cdot \dot{l} \cdot c\gamma = -\tau_f \cdot l^{-1} \cdot s\gamma \quad (12)$$

$$m \cdot \ddot{x}_{ft} - k \cdot (L-l) \cdot s\gamma + b \cdot \dot{l} \cdot s\gamma = \tau_f \cdot l^{-1} \cdot c\gamma \quad (13)$$

$$m \cdot \ddot{y}_{ft} + m \cdot g + k \cdot (L-l) \cdot c\gamma - b \cdot \dot{l} \cdot c\gamma = \tau_f \cdot l^{-1} \cdot s\gamma \quad (14)$$

where τ_f is the actuator torque during flight. During *stance*, the actuator torque is τ_s (instead of τ_f), and x_{ft} remains constant due to assumption (ii). Thus (13) can be used to calculate the static friction required for non-slip, (11) and (12) remain the same, whereas (14) becomes

$$m \cdot \ddot{y}_{ft} + m \cdot g + k \cdot (L-l) \cdot c\gamma - b \cdot \dot{l} \cdot c\gamma = \tau_s \cdot l^{-1} \cdot s\gamma + F_g \quad (15)$$

The stance phase begins with the foot initially touching the ground following a flight phase ($y_{ft} = 0$) and terminates when the force from the ground is zeroed ($F_g = 0$). During the impact of the foot with the ground, the absolute value of the coordinate y_{ft} of the foot equals the depth of penetration.

Extended MultiPart controller (x-MP). The controller objective is to achieve and retain a desired forward speed and apex height on any terrain. This controller is based on the MP presented in Section II. The leg characteristics used in the MP algorithm in order to calculate γ_{td}^j for gait j must be modified since the foot penetrates the ground and it has mass. Thus the x-MP should calculate an appropriate stiffness k' in order to compensate for this difference. To this end, the stance phase of gait $j-1$ is considered as the half period of a harmonic oscillation with natural frequency ω_s^{j-1} thus

$$\Delta t_s^{j-1} = \pi / \omega_s^{j-1} = \pi \cdot \sqrt{M/k'} \Rightarrow k' = (\pi / \Delta t_s^{j-1})^2 \cdot M \quad (16)$$

with stance duration Δt_s^{j-1} given by,

$$\Delta t_s^{j-1} = t_{lo}^{j-1} - t_{td}^{j-1} \quad (17)$$

where t_{td}^{j-1} and t_{lo}^{j-1} are the touchdown (td) and liftoff (lo) time instants. If a motion with the same characteristics was conducted on a nondeformable terrain (nd), the maximum compression of the leg's spring would have been

$$\Delta l_{max}^{j-1} = L - y_{min}^{j-1} \quad (18)$$

where y_{min}^{j-1} is the lowest height of the robot mass. Thus the leg length l_{nd}^{j-1} during stance would be approximated as

$$l_{nd}^{j-1}(t) = L - \Delta l_{max}^{j-1} \cdot \sin\left[\omega_s^{j-1} \cdot (t - t_{td}^{j-1})\right] \quad (19)$$

where $t_{td}^{j-1} \leq t \leq t_{lo}^{j-1}$ and the frequency ω_s^{j-1} can be calculated using (16).

Energy losses at the MP are introduced through the viscous damping of the leg. No energy losses occur during flight as the robot mass performs a ballistic trajectory. An appropriate damping coefficient b' must be used in the x-MP to compensate for all energy losses (leg damping and ground dissipation) that occurred during the entire gait $j-1$ duration, including flight (due to the residue oscillations). Using (19), the behavior of both models is associated. By applying energy conservation, the following applies

$$b' \cdot \int_{t_{td}^{j-1}}^{t_{lo}^{j-1}} (j_{nd}^{j-1})^2 dt = E_{gdis}^{j-1} + E_{damp}^{j-1} \quad (20)$$

where E_{gdis}^{j-1} and E_{damp}^{j-1} are the energy dissipated by the ground and by the leg's joint damping respectively. These can be calculated for the entire gait as follows

$$E_{gdis}^{j-1} = \left| \int_{t_{td}^{j-1}}^{t_{lo}^{j-1}} F_g^{j-1} \cdot \dot{y}_{ft}^{j-1} dt \right| \quad (21)$$

$$E_{damp}^{j-1} = b \cdot \int_{t_{lo}^{j-2}}^{t_{lo}^{j-1}} (\dot{l}^{j-1})^2 dt \quad (22)$$

where \dot{l} is the actual rate of leg length change. Using (16) and (20), k' and b' required in the x-MP are calculated.

The constant torque to be applied during the stance phase so as to achieve and maintain the desired forward speed is calculated in such a way that a desired energy level is reached. In the apex height of gait j (main body position at h_{des}), the system must have a desired forward speed \dot{x}_{des} . It is assumed that at the apex height, the leg spring has reached its free length L and that the leg has been positioned already at the desired touchdown angle γ_{td}^j . Thus, the desired energy level that the system must maintain in gait j is

$$E_{des}^j = \frac{1}{2}(M+m) \cdot \dot{x}_{des}^2 + M \cdot g \cdot h_{des} + m \cdot g \cdot (h_{des} - L \cdot c \gamma_{td}^j) \quad (23)$$

while the liftoff energy of the previous gait E_{lo}^{j-1} is

$$E_{lo}^{j-1} = \frac{M}{2} \cdot \left((\dot{x}_{lo}^{j-1})^2 + (\dot{y}_{lo}^{j-1})^2 \right) + \frac{m}{2} \cdot \left((\dot{x}_{ft,lo}^{j-1})^2 + (\dot{y}_{ft,lo}^{j-1})^2 \right) + M \cdot g \cdot y_{lo}^{j-1} + m \cdot g \cdot y_{ft,lo}^{j-1} + \frac{k}{2} \cdot (L - l_{lo}^{j-1})^2 \quad (24)$$

The actuator during the stance phase of gait j must compensate for the losses and maintain the motion, thus the required energy E_m^j that it must provide is

$$E_m^j = (E_{des}^j - E_{lo}^{j-1}) + E_{gdis}^{j-1} + E_{damp}^{j-1} \quad (25)$$

Due to E_m^j , the required torque τ_s^j is calculated as

$$E_m^j = \tau_s^j \cdot (\gamma_{lo}^{j-1} - \gamma_{td}^{j-1}) \Rightarrow \tau_s^j = E_m^j \cdot (\gamma_{lo}^{j-1} - \gamma_{td}^{j-1})^{-1} \quad (26)$$

If no energy losses exist, (25) and (26) show that since the controller achieves the desired values then $E_{des}^j = E_{lo}^{j-1}$ and the motion becomes an ideal oscillation and thus $\tau_s^j \approx 0$, corresponding to a passive gait.

Discussion. The development of the x-MP relies on energy magnitudes. Therefore it does not require the terrain parameters which could lead to a significantly more complex sensor system. In fact, the x-MP can easily work with the same sensors required for the MP, with the only addition of a foot force sensor to determine the ground force F_g . No extra sensors in order to determine the terrain parameters are required. Since the x-MP uses data from the previous gait, some approximate initial values must be assumed before the first gait, so that the robot be able to perform it successfully.

V. SIMULATIONS RESULTS

To evaluate the effects of the terrain and examine the behavior of the controller, a set of simulations are run. The equivalent stiffness k_g between the materials in contact (i.e. foot and ground) is used [15], where the properties of various terrains are found in [17]. For example, for a rubber foot with Young's modulus $E = 50\text{MPa}$ and granite with Young's modulus $E = 50\text{GPa}$, an equivalent stiffness of $k_g \approx 327,000\text{N/m}$ applies. Three main categories were selected compared to the leg stiffness: *soft* ground with $k_g = 8 \cdot 10^4\text{N/m}$, *moderate* ground with $k_g = 2 \cdot 10^5\text{N/m}$ and *stiff* ground with $k_g = 4 \cdot 10^5\text{N/m}$.

In all cases a monopod (Fig. 6) is considered. Its parameters are: masses $M = 4\text{kg}$ and $m = 0.1\text{kg}$, length of the leg $L = 0.30\text{m}$ and spring and damper parameters $k = 12,000\text{N/m}$ and $b = 3\text{Ns/m}$. The acceleration of gravity is 9.81m/s^2 . The simulations were performed in Matlab using ode23s with absolute and relative tolerance 10^{-5} and 10^{-4} respectively and maximum step 10^{-4} . To minimize the zero-crossing arithmetic problems created by the problem stiffness, the impact was considered over when the interaction force between the foot and the terrain was below 5N (by increasing tolerances, this value can be lower, however this set was selected as it produced both fast and reasonable results after examining various sets of tolerances).

In Fig. 7 the response of the MP and the x-MP for the defined ground types is compared. The initial conditions are: height $h_0 = 0.32\text{m}$, forward velocity $\dot{x}_0 = 1.0\text{m/s}$. The desired commands are apex height $h_{des} = 0.32\text{m} \rightarrow 0.34\text{m}$ at increments of 1cm and forward velocity $\dot{x}_{des} = 0.8\text{m/s}$, while the ground is becoming more compliant. The figure is divided in the three regions according to stiffness. When the ground is stiff, the MP tries to achieve the objectives however the desired velocity is not reached, while the x-MP quickly converges to the desired values. In the moderate ground the MP reaches again a steady state, however not at the desired values, while the x-MP quickly adapts.

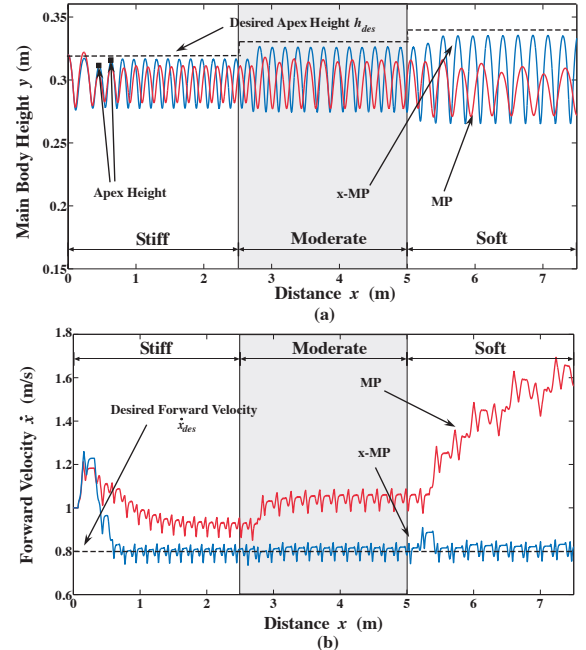


Figure 7. MP & x-MP comparison for (a) Apex height (b) Forward velocity.

As the ground becomes soft the MP is destabilized; again the x-MP follows the desired commands. Note that the MP performs better as the ground can be assumed as nondeformable, i.e. $k_g \rightarrow (\geq 10^6 \text{ N/m})$. As compliance increases the MP is destabilized as it disregards the effects of energy losses. This is due to the fact that the exact mechanics of the impact between the foot and the ground are disregarded in the control design; the MP assumes no energy losses occur in stance due to the ground compliance. On the other hand the x-MP adapts quickly to each terrain and maintains its performance independently of the ground.

Finally the performance of the x-MP is presented in Fig. 8 for various terrains where except for different compliances (shown by different k_g), shape deformation also exists using (8) (shown by the $\max \lambda = a(i)$ in the figure). The initial conditions are height $h_0 = 0.33\text{m}$ and forward velocity $\dot{x}_0 = 1.0\text{m/s}$ and the goals are apex height $h_{des} = 0.32\text{m}$ and forward velocity $\dot{x}_{des} = 0.8\text{m/s}$. At the beginning in the stiff terrain the x-MP adapts quickly. Next as the ground softens and the deformations increase, more torque is required to achieve the desired values. As the deformations become larger ($\max \lambda = 3$) the x-MP results in small deviations, due to the fact that on such terrain k' and b' do not fully compensate the deformations; the improvement of the controller on such cases is an ongoing work. At the moderate ground, the torque requirements are lower, however again the effect of the higher deformation is obvious.

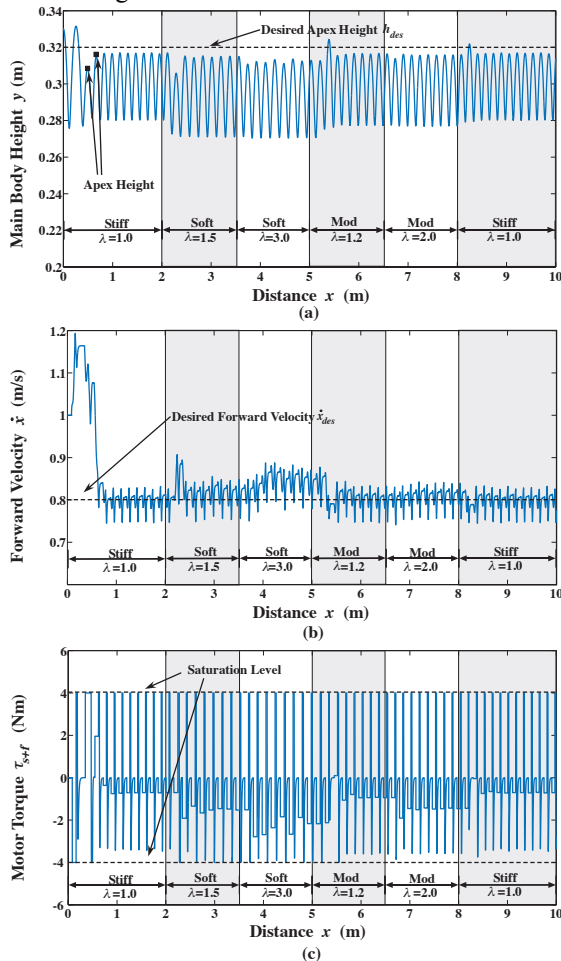


Figure 8. Monopod run on a terrain with various values using x-MP: (a) Apex height, (b) Forward velocity and (c) Motor torque.

Yet x-MP retains its desired values and finally as the robot enters again the stiff terrain, it can easier achieve the goals. The torque during stance is between 0Nm and -3Nm .

VI. CONCLUSIONS

This work studied the effects of foot-terrain interactions in legged robots and control methods to cancel them out. The adverse effects of terrain deformation during motion were illustrated and a new model for impact dynamics was developed, allowing the study of the behavior of a monopod robot in fast walking. Based on previous response monitoring, the MP controller was modified to cope with deformable terrains. The new controller, called x-MP, does not require an exact knowledge of terrain parameters and still compensates for the effects of the energy losses. Using the x-MP, the system was able to overcome the variations of the ground, stabilizing the gait characteristics near the desired ones. In the ongoing work, extension of this work to include further leg and terrain details, tangential forces, cost of transport and experiments, is underway.

REFERENCES

- [1] McGhee, R.B. and Iswandhi, G.I., "Adaptive Locomotion of a Multilegged Robot over Rough Terrain", *IEEE Transactions on Systems, Man and Cybernetics*, vol. 9, pp. 176-182, 1979.
- [2] Hodgins, J., "Legged Robots on Rough Terrain: Experiments in Adjusting Step Length", *IEEE Int. Conf. on Robotics and Automation*, Philadelphia, PA, pp. 824-826., 1988.
- [3] Saranli, U., Buehler, M. and Koditschek, D.E., "RHex: A Simple and Highly Mobile Hexapod Robot", *The Int. Journal of Robotics Research*, vol. 20, pp. 616-631, 2001.
- [4] Buehler, M., Playter, R. and Raibert, M., "Robots Step Outside", in *Int. Symp. Adaptive Motion of Animals and Machines*, Ilmenau, 2005.
- [5] Berkemeier, M.D. and Fearing, R.S., "Sliding and hopping gaits for the underactuated acrobot," *IEEE Tr. Robot. Autom.* 14(4), pp. 629-634, 1998.
- [6] Cherouveim, N. and Papadopoulos, E., "Control of Hopping Speed and Height Over Unknown Rough Terrain Using a Single Actuator," *Proc. IEEE International Conference on Robotics and Automation (ICRA '09)*, Kobe, Japan, pp. 2743-2748, May 2009.
- [7] Ding, L. et al, "Foot-Terrain Interaction Mechanics for Legged Robots: Modeling and Experimental Validation," *The International Journal of Robotics Research*, 2013.
- [8] Wong, J. Y., *Terramechanics and Off-road Vehicle Engineering*, 2nd Edition, Elsevier Ltd., 2010.
- [9] Li, C., Zhang, T., and Goldman, D.I., "A teradynamics of legged locomotion on granular media," *Science*, 339(6126), pp. 1408-1412, 2013.
- [10] Gilardi, G. and Sharf, I., "Literature Survey of Contact Dynamics Modelling," *Mechanism & Machine Th.*, 37(10), pp. 1213-1239, 2002.
- [11] Stronge, W. J., *Impact Mechanics*, Cambridge Univ. Press, 2000.
- [12] Yigit, A. S., Christoforou, A. P., and Majeed, M. A., "A nonlinear visco-elastoplastic impact model and the coefficient of restitution," *Nonlinear Dynamics*, 66(4), pp. 509-521, 2011.
- [13] Kontolatis, I. et al, "Quadruped optimum gaits analysis for planetary exploration," *12th Symposium on Advanced Space Technologies in Robotics and Automation*, (ASTRA '13), ESA, Noordwijk, 2013.
- [14] Nikolakakis, A. et al, "Implementation of a Quadruped Robot Pronking/ Bounding Gait Using a Multipart Controller," *Dynamic Systems and Control Conference*, Cambridge, MA, USA, 2010.
- [15] Johnson, K. L., *Contact mechanics*. Cambridge Univ. Press, 1977.
- [16] Marhefka ,D. W. and Orin, D. E., "A compliant contact model with nonlinear damping for simulation of robotic systems," *IEEE Transactions on Systems, Man, and Cybernetics-part A: Systems and Humans*, vol. 29, no. 6, pp. 566-572, 1999.
- [17] <http://www.stanford.edu/~tyzhu/Documents/Some%20Useful%20Numbers.pdf>.